Reflectionless standing-wave operation in microring resonators

Kenaish Al Qubaisi[1,*], Đorđe Gluhović[1], Deniz Onural[1], and Miloš A. Popović[1,†]

[1]*Department of Electrical and Computer Engineering, Boston University, Boston, MA 02215, USA*

[*]*kalqubai@bu.edu,* [†]*mpopovic@bu.edu*

Abstract: We demonstrate a scheme for microring resonators to operate as standing-wave resonators while eliminating reflections and maintaining traveling-wave-resonator-like through-port response, potentially enabling interdigitated *p-n* junction microring modulators to achieve higher performance than other junction geometries.

The resonant nature, smaller footprint, and higher energy efficiency of microring resonator based active devices (as compared to their Mach-Zehnder interferometer counterparts) has enabled on-chip optical links with a larger number of wavelength-division multiplexed (WDM) channels. Combining this with the dense integration of a large number of electronic and photonic devices on the same chip has led to the recent demonstration of integrated optical links with bandwidth density exceeding 1 Tbps/mm^2 and a low energy cost of 0.83 pJ/bit [1].

Coupling of the forward and backward propagating modes in microring resonators, due to sidewall roughness and/or via the ring-bus directional coupler, can potentially be detrimental to the performance of various microring-based devices such as modulators or sensors [2, 3], and can lead to resonance splitting. Approaches for eliminating such splitting have been proposed, e.g. by including a tunable reflector within the resonator structure. This comes at a cost of increasing the resonator's footprint and complexity, simultaneously lowering its free-spectral range (FSR) [4].

A scheme to improve the performance of microring modulators with interdigitated *p-n* junctions by employing standing-wave operation has been proposed by us in [5]. It takes advantage of a unique alignment between azimuthally distributed pn junctions and the nodes of a ring resonator optical mode, possible only in this junction geometry. By matching the longitudinal standing-wave resonance mode nodes with the high doping concentration regions within the microring, both the quality factor and modulation efficiency of the device are improved compared to an identical traveling-wave microring modulator. This is because the high-carrier-concentration regions that carry charge to the junctions do not contribute to modulation within the modulator, yet they incur optical loss via free-carrier absorption in a traveling-wave microring modulator. In the standing wave version, these regions mostly overlap field nulls of the optical mode, while the junctions have better overlap with field peaks. However, inherent to the standing-wave operation of a ring resonator (e.g. induced by a sidewall grating) is the coupling of a portion of the light within the resonator back into the input port. This occurs in the otherwise standard side-coupled-bus ring modulator configuration, useful for WDM cascading. Such reflections are undesirable in WDM systems and require either a circulator or a large footprint and complex interferometer to eliminate them [5, 6]. They also may require a larger linewidth for the same intrinsic Q.

In this paper we demonstrate a resonator scheme that operates microring cavities in standing-wave regime, yet eliminate reflections, in a footprint and energy conscious manner, making them suitable as building blocks of on-chip WDM links. The device concept is depicted in Fig. 1(a) and is composed of two microring cavities, aligned horizontally center-to-center, are placed on opposite sides of the bus waveguide. The radius of the microrings is 5 μm and the starting ring waveguide width is 500 nm. A sinusoidal corrugation is added to both sides of the ring waveguide with peak-to-peak of 50 nm, such that at its maximum the width of the waveguide is 600 nm and 500 nm at its minimum. The cavities are designed to operate near 1550 nm. They have an interior ridge, i.e the microring's waveguide is fully etched on the outer edge and is partially etched on the interior edge. Fully thickness waveguide sections are illustrated with light

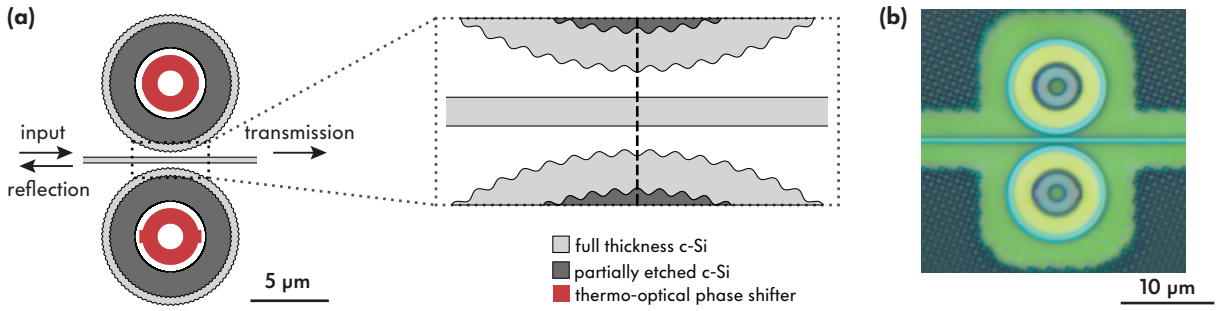

Fig. 1: (a) Geometry of the dual standing-wave microring resonators as laid out on the design mask. The inset shows the relative orientation of of the sidewall corrugations between the top and bottom microrings. (b) Optical micrograph of the device.

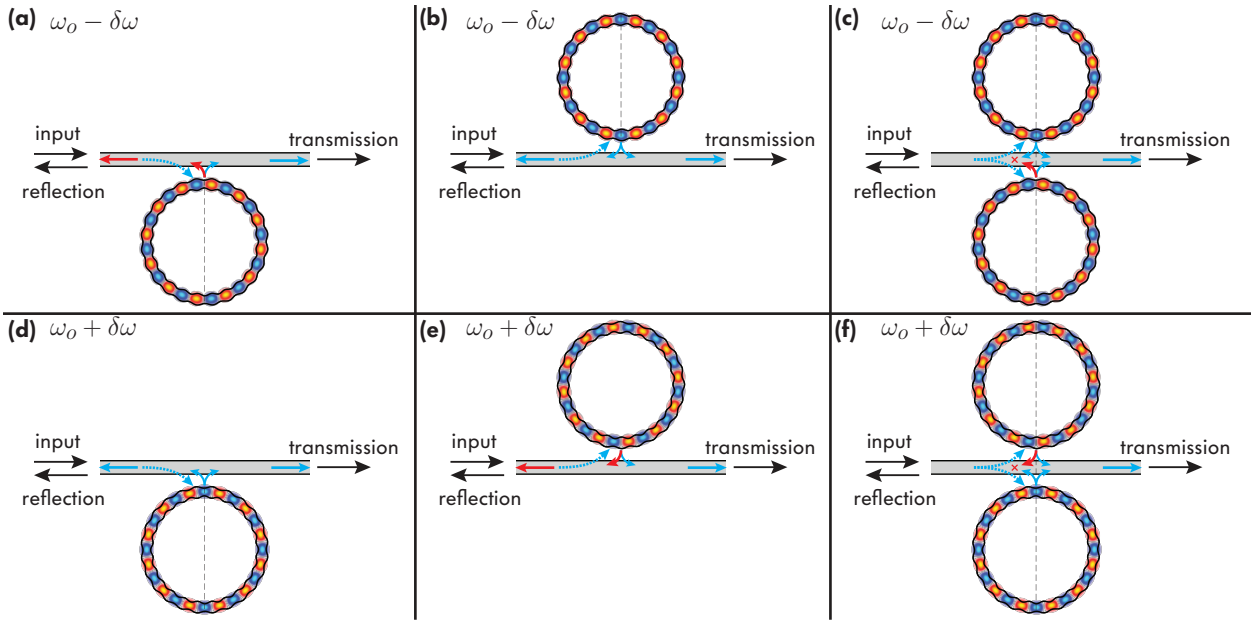

Fig. 2: The electric field profile of the longitudinal standing-wave resonance modes at the lower resonance frequency $\omega_o - \delta\omega$ for: (a) bottom microring resonator with anti-symmetric field profile, (b) top microring resonator with symmetric field profile, and (c) both microring resonators which also illustrates how the reflection is canceled in the bus waveguide. Similarly for the longitudinal standing-wave resonance modes at the higher resonance frequency $\omega_o + \delta\omega$ (d) shows bottom microring resonator with symmetric field profile, (e) shows top microring resonator with anti-symmetric field profile, and (f) shows both microring resonators and the cancellation of the reflection due to destructive interference.

grey color in Fig. 1(a) and can be seen in light blue color in the optical micrograph in Fig. 1(b). Similarly, partially etched, thinner silicon is illustrated with dark grey color in Fig. 1(a) and can be seen in light yellow color in Fig. 1(b). The two microrings are identical with the exception that one is rotated by half a sinusoidal period with respect to the other ring. Each microring has a thermo-optical phase shifter, placed in the inner region of the ring, used to align the resonance frequencies of the two cavities to each other. The device was fabricated in the new GlobalFoundries 45CLO 45 nm-node monolithic electronics-photonics CMOS platform optimized for silicon photonics [7].

The principle of operation of the device is depicted in Fig. 2. The corrugations added to the sides of the waveguide cause the forward propagating mode in the resonator to be coupled to the backward propagating mode, thereby breaking their degeneracy and causing resonance frequency splitting into two standing-wave modes with opposite mode symmetries. One is at a lower resonance frequency $\omega_o - \delta\omega$ while the other is at a higher resonance frequency $\omega_o + \delta\omega$. The larger the coupling between the forward and backward propagating modes, the larger the frequency splitting $2\delta\omega$ between the two standing-wave resonance modes. Therefore, our two ring system has a total of four standing-wave resonance, compared to just two traveling-wave resonance modes (being excited) if there were no corrugations and/or no reflections within the microrings. When the resonance frequencies of both rings are aligned to ω_o, the relative rotation the bottom microring resonator by half the sinusoidal corrugation period results in the standing-wave fields to be rotated by $\lambda_o/4$ with respect to the top microring resulting in standing-waves with opposite mode symmetry at a given resonance frequency. This causes the reflected light waves from the two cavities to destructively interfere when coupling into the bus waveguide, while forward propagating light constructively interfere into the bus, effectively restoring the traveling wave behaviour of conventional microring resonators while maintaining standing wave operation in each ring. Also, due to the symmetry mismatch between the standing-wave resonance modes in the two microring, there is no direct or indirect (via the bus waveguide) coupling between the modes of opposite cavities.

This is an extension of an idea applied and demonstrated recently [6] for 1D photonic crystal (PhC) nanobeam cavities. However, a major distinction between a PhC nanobeam cavity and a microring resonator with standing-wave operation is that a microring has two standing resonance modes, while the PhC nanobeam cavity has just one resonance near the frequency of interest. Therefore, the linewidths of individual resonance modes (a function of cavity loss and power coupling to the bus waveguide) and the amount of frequency splitting between the two standing wave resonance modes (a function of corrugation strength) has to be matched in order for the four resonance modes to coalesce into a single resonance mode with traveling-wave behaviour.

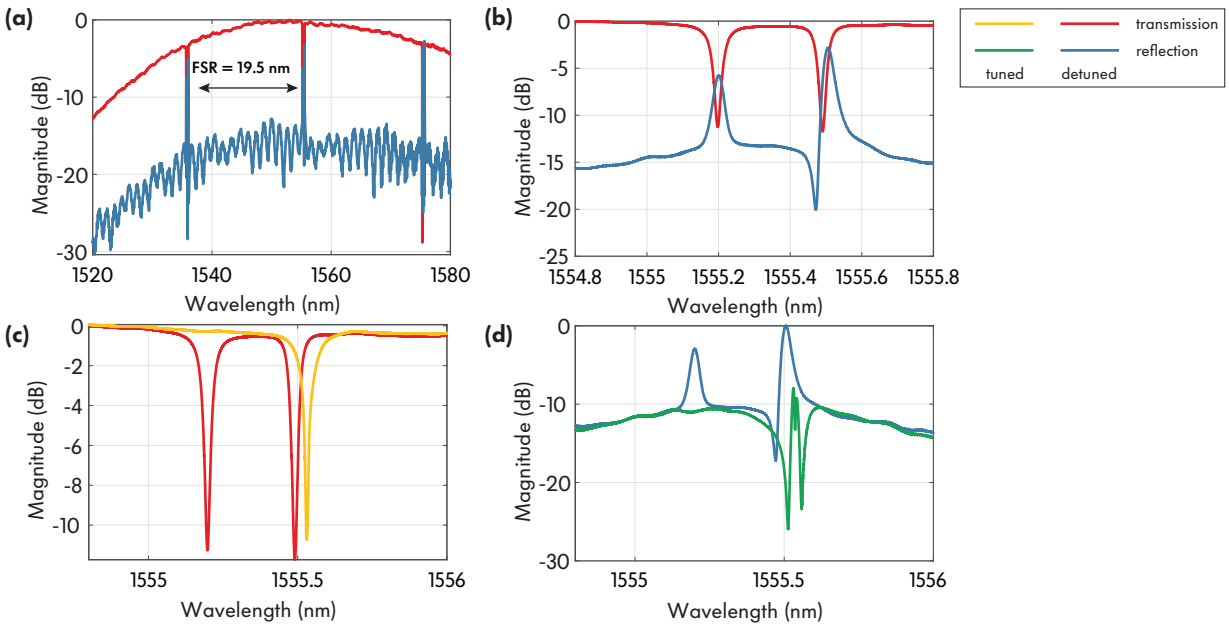

Fig. 3: (a) Wide spectra of the transmission and the reflection when the device when the microring resonators are detuned. (b) Transmission and reflection in the vicinity of 1555 nm. (c) Transmission response when the microring resonators are detuned (red) and after tuning (yellow). (d) Reflection response when the microring resonators are detuned (blue) and after tuning (green).

Fig. 3 shows the measurement results of the device in the detuned and tuned states. The FSR was measured to be 19.5 nm as seen in Fig. 3(a). Additionally, the two microring resonators are initially misaligned about 0.29 nm (36.3 GHz). There is no visible corrugation in induced splitting between the two standing wave modes in each cavity because they are overcoupled. The gap between the bus waveguide and each ring was set to 250 nm. The resulting over-coupling to the bus waveguide is consistent with the strong reflection response [6] seen in Fig. 3(b). Furthermore, in the detuned state, the linewidths of the resonances are around 5.3 GHz which corresponds to a total quality factor Q of 36,340. The heater of the bottom microring was actuated (0.45 V, 2.75 mW) to red-shift the resonance wavelength of the bottom ring by 0.33 nm thereby aligning both resonators to the same resonance frequency as shown in Fig. 3(c). When tuned, the linewidth of the resonance was 3.9 GHz which corresponds to a Q of 49,000 and with a 1 dB reduction in the extinction ratio compared to the maximum extinction ratio in the detuned state. When tuned the maximum reflection was decreased by 8 dB, almost matching the noise floor as seen in Fig. 3(d), and achieving near reflectionless operation.

In conclusion, we demonstrated a reflectionless microring resonator unit with two microrings operating as standing-wave cavities. Further, we carried out the demonstration in an advanced monolithic electronic-photonic platform, compatible with both active silicon cavities like ring modulators, and electronics integration. Unlike the approach in [4], the presented scheme does not diminish the FSR of the microring resonators and allows for standing-wave operation while simultaneously maintaining the traveling-wave aspects desirable for on-chip WDM links. We believe that this scheme is a promising approach to harness the benefits of standing-wave operation in active devices, and in particular in microring resonators, a regime of operation which thus far has been underutilized. For instance, it could potentially lead to an optimum geometry for microring modulators with interdigitated *p-n* junctions in terms of modulation efficiency [5].

Acknowledgments: We thank the GlobalFoundries 45CLO process team and Ayar Labs, Inc. for extensive support and interaction. Fabricated on the Shasta test vehicle. Funding: National Science Foundation Award #2023751 (ASCENT) and a fellowship from the Abu Dhabi National Oil Company.

References

1. M. Wade *et al.*, "A bandwidth-dense, low power electronic-photonic platform ..." *2018 (ECOC)*. IEEE, 2018.
2. Little, Brent E., Juha-Pekka Laine, and Sai T. Chu. "Surface-roughness-induced contradirectional coupling ..." *Optics letters* 22.1 (1997).
3. Li, Ang, et al. "Backscattering in silicon microring resonators: a quantitative analysis." *Laser & Photonics Reviews* 10.3 (2016): 420-431.
4. Li, Ang, and Wim Bogaerts. "Fundamental suppression of backscattering in silicon microrings." *Optics express* 25.3 (2017): 2092-2099.
5. Pavanello, Fabio, et al. "Ring modulators with enhanced efficiency based on standing-wave operation ..." Optics express 24.24 (2016).
6. Al Qubaisi, Kenaish, and Miloš A. Popović. "Reflectionless dual standing-wave microcavity resonator units ..." Optics Express 28.24 (2020).
7. Rakowski, Michal, et al. "45nm CMOS-silicon photonics monolithic technology (45CLO) for next-generation ..." OFC 2020.